Appl Water Sci (2017) 7:1131–1150
DOI 10.1007/s13201-017-0540-6

ORIGINAL ARTICLE

Application of multivariate statistical technique for hydrogeochemical assessment of groundwater within the Lower Pra Basin, Ghana

C. K. Tay[1] · E. K. Hayford[2] · I. O. A. Hodgson[1]

Received: 5 June 2013 / Accepted: 1 February 2017 / Published online: 22 February 2017

Abstract Multivariate statistical technique and hydrogeochemical approach were employed for groundwater assessment within the Lower Pra Basin. The main objective was to delineate the main processes that are responsible for the water chemistry and pollution of groundwater within the basin. Fifty-four (54) (No) boreholes were sampled in January 2012 for quality assessment. PCA using Varimax with Kaiser Normalization method of extraction for both rotated space and component matrix have been applied to the data. Results show that Spearman's correlation matrix of major ions revealed expected process-based relationships derived mainly from the geochemical processes, such as ion-exchange and silicate/aluminosilicate weathering within the aquifer. Three main principal components influence the water chemistry and pollution of groundwater within the basin. The three principal components have accounted for approximately 79% of the total variance in the hydrochemical data. Component 1 delineates the main natural processes (water–soil–rock interactions) through which groundwater within the basin acquires its chemical characteristics, Component 2 delineates the incongruent dissolution of silicate/aluminosilicates, while Component 3 delineates the prevalence of pollution principally from agricultural input as well as trace metal mobilization in groundwater within the basin. The loadings and score plots of the first two PCs show grouping pattern which indicates the strength of the mutual relation among the hydrochemical variables. In terms of proper management and development of groundwater within the basin, communities, where intense agriculture is taking place, should be monitored and protected from agricultural activities. especially where inorganic fertilizers are used by creating buffer zones. Monitoring of the water quality especially the water pH is recommended to ensure the acid neutralizing potential of groundwater within the basin thereby, curtailing further trace metal mobilization processes in groundwater within the basin.

Keywords Groundwater pollution · Hydrogeochemical processes · Principal component analysis (PCA) · Lower Pra Basin · Ghana

Introduction

Globally, groundwater is a fundamental natural resource for the provision of drinking water, and plays a critical role in the quest for sustainable human life, as it is estimated that approximately, 30% of the world's freshwater is stocked as groundwater with about 97% of all freshwater being potentially available for human use (Morris et al. 2003). In Africa, including Ghana, majority of the populations who depend on groundwater for domestic purposes, live in rural and peri-urban communities, where poverty predominates. Lack of access to quality groundwater in these communities in Africa, therefore, not only infringes on their basic human rights but also impact negatively on sustainable human life. Since the last decades, African governments have continually taken measures to provide their people with quality water from groundwater sources, due to the fact that, groundwater is not only feasible but also the most economical source of potable water for

✉ C. K. Tay
collinstay@hotmail.com; korblatay@yahoo.co.uk

[1] Council for Scientific and Industrial Research-Water Research Institute, P.O. Box AH 38, Achimota, Accra, Ghana

[2] Department of Earth Science, University of Ghana, Legon, Accra, Ghana

scattered and remote communities (Duah 2007). It is thus, paramount to ensure the management and development of groundwater within the rural communities to ensure sustainability.

During the past decades, interest in the geochemistry of groundwater has increased as demonstrated by several hydrogeochemical studies which are increasingly becoming a firm part of regional hydrogeological studies. Earlier studies on the categorization of groundwater facies and chemical evolutionary history employed graphical presentations of major-ion composition of groundwater (Piper 1944; Stiff 1951; Schoeller 1965; Hem 1989). These schemes were useful in visually describing differences in major-ion chemistry of groundwater and categorizing water compositions into identifiable groups which are usually of similar genetic history (Freeze and Cherry 1979).

Recently, multivariate statistical technique for hydrogeochemical assessment of groundwater has been applied with remarkable success as a tool in the study of groundwater chemistry. The application of multivariate statistical methods to geo-environmental data sets have facilitated the unveiling of hidden structures in the data sets and assisted in resolving key geo-environmental problems at various scales (Sandaw et al. 2012). Multivariate analysis of geochemical data operated on the concept that each aquifer zone has its own unique groundwater quality signature, based upon the chemical makeup of the sediments that comprise it (Fetter 1994; Suk and Lee 1999; Woocay and Walton 2008). The application of statistical analysis thus helps in the interpretation of complex data matrices to better understand the water quality as well as identify the possible factors that influence the water chemistry in a region.

Earlier examples of classical applications of multivariate statistical methods in the earth sciences are contained in Guler et al. (2002), Cloutier et al. (2008), Jiang et al. (2009) and Kim et al. (2009), the delineation of zones of natural recharge to groundwater in the Floridan aquifer (Lawrence and Upchurch 1982), the delineation of areas prone to salinity hazard in Chitravati watershed of India (Briz-Kishore and Murali 1992), characterization of groundwater contamination using factor analysis (Subbarao et al. 1995), analysis of marine water quality and source identification (Zhou et al. 2007), and the resolution of simple geo-environmental problems in the determination of groundwater flow directions (Farnham et al. 2003). The effectiveness of this method in groundwater chemistry over the traditional piper and stiff schemes stems from its ability to further reveal hidden inter-variable relationships and allow the use of virtually limitless numbers of variable, thus trace elements and physical parameters can be part of the classification parameters. By its use of raw data as variable inputs, errors arising from close number systems (mutual relation between variables with similar characteristics) are avoided. In addition, because elements are treated as independent variables, the masking effect of chemically similar elements that are often grouped together is avoided (Dalton and Upchurch 1978).

Owing to the discharge of mine effluents into river and stream sources through mining activities, several of the surface water resources which hitherto, served as potable sources for the communities within the Lower Pra Basin, have become polluted and unsuitable for use as drinking and potable water supply. Communities within the basin thus rely heavily on groundwater as sources for drinking and domestic purposes. However, sulphide rocks that contain gold ore, which is prevalent in the area often contain pyrite and arsenopyrites. Exposure of these rocks to the atmosphere often results in acid mine drainage generation (low pH waters) and subsequent mobilization of trace metals in high proportions into the groundwater system. The indiscriminate use of Hg and other chemicals through "small-scale" mining activities within the basin also lead to the pollution of surface- and groundwater resources. The resultant of all these is the change in the characteristics of both surface-and groundwater resources which serve as sources of potable water supply to the communities that rely on them. Earlier studies within the basin include: Catchment-Based Monitoring Project in Ghana-National IWRM Plan (2010), Ahialey et al. (2010), Bayitse (2011) and Tay et al. (2014, 2015). These studies failed to apply multivariate statistical methods to unveil the hidden structures and subsequently delineate the factors responsible for groundwater pollution within the Lower Pra Basin.

It is against this background that, this paper seeks to apply multivariate statistical analysis as a tool for a comprehensive hydrogeochemical assessment of groundwater in order to facilitate the unveiling of hidden structures in the data sets and assist in delineating the factors responsible for groundwater pollution for proper development and management of groundwater within the basin.

Materials and methods

Description of the study area

The Lower Pra Basin lies between 05°0′0″ and 06°0′0″N and 01°0′0″ and 02°0′0″W (Fig. 1). The climate falls under the wet semi-equatorial climatic zone of Ghana (Dickson and Benneh 1980). The basin comes strongly under the influence of the moist south-west monsoons during the rainy season. It is quite humid (relative humidity 60–95%) with annual rainfall in the range of 1500–2000 mm (Dickson and Benneh 1980). The average minimum and

Fig. 1 Map of the study area (Ghana map *inset*) showing sampling communities within the various geological setting of the Lower Pra Basin

maximum temperatures are 21 and 32 °C, respectively (Dickson and Benneh 1980). The Pra Basin is part of the south-western basin system in Ghana and has a drainage area of 23,188 km^2 and an estimated mean annual discharge of 214 $m^3\ s^{-1}$ (Dickson and Benneh 1980). The basin lies entirely within the Forest Ecological Zone in Ghana (Dickson and Benneh 1980). It has moist semi-deciduous forest with valuable timber species (Dickson and Benneh 1980). Due to the expansion of the cocoa industry the original forest has changed to a secondary forest consisting of climbers, shrubs and soft woody plants (Dickson and Benneh 1980). Many trees in the upper and middle layers exhibit deciduous characteristics (Dickson and Benneh 1980). The basin is principally dominated by the forest orchrosols, and to a lesser extent, the forest orchrosol–oxysol integrate. The orchrosols are highly coloured soils with little leaching characteristics (Dickson and Benneh 1980).

Land use

The land use pattern within the basin is primarily, farming (cocoa and food crops) and gold mining. Large acreages of virgin forest were removed and replaced with cocoa farms. In addition, food crops, such as cassava, yam, cocoyam, plantain, as well as fruits, such as banana; oranges etc, are produced together with cocoa for subsistence. Gold mining within the basin is of two types, "large-scale" and "small-scale" ("*Galamsey*"). "Large-scale" mining is conducted by heap leach technique or roasting of ore. Oxidised ores derived from sulphide principally arsenopyrites, realgar, orpiment, and pyrites in the weathered zones are heap leached by cyanidation (Kortatsi 2007). Paleoplacer (free milling ore) is mined from deep zones crushed, milled, and cyanided (Kortatsi 2007). "Small-scale" mining involves extracting gold from ochrosols soils mainly from stream floors by mercury amalgamation (Kortatsi 2007).

Geology

The Basin is characterized primarily by Cape Coast granitoid complex and a small percentage of Dixcove granitoid complex. Some portion of the basin is also characterized by Birimian and Tarkwaian Systems.

Cape Coast granitoid

Most part of the Cape Coast granitoid complex is predominantly granitic to quartz dioritic gneiss, which in the field is seen to change gradually from fine to medium grained, foliated biotite quartz diorite gneiss to exclusively hornblende-guartz-diorite gneiss (Ahmed et al. 1977). The gneissic rocks are interrupted by acidic and basic igneous rocks, such as white and pink pegmatite, aplites granodiorites, and dykes (Ahmed et al. 1977). Typically, the granitoids are associated with many enclaves of schists and gneisses. The Cape Coast granitic units are sometimes well foliated and often magmatic potash-rich granitoids in the form of muscovite, biotite, granite and granodiorite, granodiorites biotite gneiss, aplites and pegmatites (Ahmed et al. 1977). They are usually associated with Birimian metasediments and their inner structure is always concordant with those of their host rocks (Ahmed et al. 1977). The Cape Coast granitoid complex is believed to symbolize a multiphase intrusion comprising of four separate magmatic pulses. The last phase of the magmatic pulses is believed to be associated with the upper group of Birimian metasediments (Ahmed et al. 1977). The general mineralogical composition of the Cape Coast granitoid complex includes quartz, muscovite, biotite, microcline, albite, almandine, beryl, spessartite, tourmaline, columbite/tantalite and kaolin (Kesse 1985).

Dixcove granitoid

This complex consist of hornblende granite or granodiorite grading locally into quartz diorite and hornblende diorite, sometimes believed to have been formed from gabbros by magmatic differentiation (Ahmed et al. 1977). This complex forms non-foliated discordant to semi-discordant bodies in the enclosing country rocks which are generally Upper Birimian metavolcanics, numerous enclaves of which are found within the granite complex (Ahmed et al. 1977). The Dixcove granitoid complex is intruded along deep seated faults in three distinct phases which follow one another from basic to acid gabbrodiorite–granodiorite (Ahmed et al. 1977).

Birimian supergroup

The Birimian supergroup comprises the Lower and Upper Birimian and is separated from the Tarkwaian system by a major unconformity (Kesse 1985). The Lower Birimian is principally pelitic in origin having muds and silts with beds of coarser sediments (Kesse 1985). The Upper Birimian is predominantly of volcanic and pyroclastic origin (Kesse 1985). The rocks consist of bedded group of green lavas (greenstones), tuffs, and sediments with minor bands of phyllite that comprise a zone of manganiferous phyllites containing manganese ore (Kesse 1985). The sequence is intruded by batholithic masses of granite and gneiss (Kesse 1985). These principally argillaceous sediments were metamorphosed to schist, slate and phyllite, with some interbedded greywacke (Kesse 1985).

The Tarkwaian

The Tarkwaian consists of an overall fining-upwards thick clastic sequence of argillaceous and arenaceous sediments (mainly arenaceous) with two well-define zones of pebbly beds and conglomerate in the lower members of the system (Junner et al. 1942). The Tarkwaian rocks comprise slightly metamorphosed shallow-water, sedimentary strata, predominantly sandstone, quartzite, shale and conglomerate resting unconformably on and derived from rocks of the Birimian supergroup (Junner et al. 1942).

Aquifer characteristics

Boreholes within the basin are generally shallow with depths which ranged 22–96 m and a mean value of 44.42 m. Borehole yield is generally low and largely variable, ranging from 0.4 to 51.7 $m^3\ h^{-1}$ with a mean value of 4.55 $m^3\ h^{-1}$, with schists and granite aquifers having relatively higher yields. The fractures in the rocks are generally open. The granite and schist rocks are exposed, while, the Birimian and Tarkwian rocks have thick overburdens. The soils develop over the same kind of highly weathered parent material with lateritic to clayey top soil layer and thickness which generally ranged 4–14 m. However, the soil layer thickness may extend further in some areas. The static water levels of the boreholes generally ranged 0.4–22.4 m with a mean value of 6.37 m. Static water levels in most boreholes are above the top of the aquifer suggesting that the aquifers are either confined or semi-confined. The gneiss and granite associated with the Birimian rocks are of significant importance to the water economy of Ghana, since they underlie extensive and often well-populated areas (Dappah and Gyau-Boakye 2000). They are not inherently permeable, but secondary permeability and porosity have developed as a result of fracturing and weathering (Dappah and Gyau-Boakye 2000). Where, precipitation is high and weathering processes penetrate deeply along fracture systems, the granite and gneiss commonly have been eroded down to low-lying areas (Dappah and Gyau-Boakye 2000). On the other hand, where, the

precipitation is relatively low, the granite occurs in massive poorly jointed inselbergs that rise above the surrounding lowlands (Dappah and Gyau-Boakye 2000). In some areas, weathered granite or gneiss form permeable groundwater reservoir (Dappah and Gyau-Boakye 2000). Major fault zones are also favourable locations for groundwater storage (Dappah and Gyau-Boakye 2000). The Birimian phyllite, schist, slate, greywacke, tuff, and lava are generally strongly foliated and fractured. Where, they crop out or are near the surface, considerable water may percolate through them (Dappah and Gyau-Boakye 2000).

Sampling and laboratory analysis

Fifty-four (54) (No) groundwater samples were collected from boreholes in January 2012 for quality assessment. Sampling protocols described by (Claasen 1982) and (Barcelona et al. 1985) were strictly observed during sample collection. Samples were collected using 4-1 acid-washed polypropylene containers. The samples were collected into 1 L polyethylene bottles without preservation. Samples for trace metals analyses were acidified to a pH <2 after filtration (Appelo and Postma 1999). All samples were stored on ice in an ice-chest. Samples for physico-chemical analyses were transported to the CSIR-Water Research Institute laboratories in Accra, stored in a refrigerator at a temperature of <4 °C and analyzed within 1 week. Temperature, pH, and electrical conductivity were measured on site using Hach Sens ion 156 m. Chemical analyses of the samples were carried out using appropriate certified and acceptable international procedures outlined in the Standard Methods for the Examination of Water and Wastewater (APHA 1998); sodium (Na) was analysed by flame photometric method; calcium (Ca) by EDTA titration; TDS by gravimetric method; Magnesium (Mg) by calculation after EDTA titration of calcium and total hardness; chloride (Cl) by argentometric titration; Nitrate-nitrogen was analysed by hydrazine reduction and spectrophotometric determination at 520 nm. Analyses of trace elements excluding arsenic and mercury were carried out using Unicam 969 Atomic Absorption Spectrophotometer (AAS), arsenic (As) determination was carried out using an ARL 341 hydride-generator), while, mercury (Hg) was determined using the cold vapour method at the Metals Section of the Environmental Chemistry and Sanitation Engineering Division laboratories of the Council for Scientific and Industrial Research-Water Research Institute (CSIR-WRI) in Accra. An ionic error balance was computed for each chemical sample and used as a basis for checking analytical results. In accordance with international standards, results with ionic balance errors greater that 5% were rejected (Appelo and Postma 1999). Charge balances were calculated using Eq. (1):

$$\mathrm{CB} = \left[\left(\sum zM_{\mathrm{c}} - \sum zM_{\mathrm{a}}\right) / \left(\sum zM_{\mathrm{c}} + \sum zM_{\mathrm{a}}\right)\right] \times 100 \quad (1)$$

where z is the ionic charge, M is the molality, and the subscripts a and c refer to anions and cations, respectively.

Spearman's correlation matrix

Coefficient of correlation (r) was used to understand the relationship between the various parameters and to test the significance of the models. The Spearman's correlation matrix was generated using Statistical Programme for Social Sciences (SPSS) 16.0 for windows. Correlation matrix was studied to point out any relationship between the observed parameters in order to explain factor loadings during PCA. In other words, correlation matrix was utilized to point out the internal structures and assist in the identification of pollution sources not accessible at first glance (Satheeshkumar and Anisa Khan 2011). High correlation coefficient value (i.e., −1 or 1) predicts a good relation between two variables and correlation coefficient value around zero (0) predicts no relationship between the two variables at a significant level of $P < 0.05$. Parameters showing $r > 0.7$ are considered to be strongly correlated whereas r between 0.4 and 0.7 shows moderate correlation and parameters showing $r < 0.4$ shows low to no correlation.

Principal component analysis (PCA)

PCA is a very powerful technique used to reduce the dimensionality of a data set consisting of a large number of interrelated variables while retaining as much as possible the variability presented in a data set (Zhang et al. 2009). The reduction is achieved by transporting the data set into a new set of variables- the principal components (PCs), which are orthogonal (non-correlated) and are arranged in decreasing order of importance (Zhang et al. 2009). PCA technique extracts the eigenvalues and eigenvectors from the covariance matrix of original variables. PCA is designed to transform the original variables into new, uncorrelated variables (axes), called the principal components, which are linear combinations of the original variables. The new axes lie along the directions of maximum variance (Shrestha and Kazama 2007). PCA reduces the dimensionality of the data set by explaining the correlation amongst large number of variables in terms of a smaller number of underlying factors without losing much information (Vega et al. 1998; Alberto et al. 2001). PCA can be expressed mathematically as presented in Eq. (2):

$$Z_{ij} = pc_{i1}x_{1j} + pc_{i2}x_{2j} + \cdots pc_{im}x_{mj} \quad (2)$$

where z is the component score, pc is the component loading, x is the measured value of the variable, i is the

component number, j is the sample number, and m is the total number of variables.

Statistical analysis

Statistical analyses were performed using SPSS 16.0 for windows. PCA technique was used to reduce the dimensionality of the data set while retaining the variability presented in a data set as much as possible. The Spearman's correlation matrix was generated to determine any relationship between the observed parameters in order to explain factor loadings during PCA. In order to ensure normality of the data, all hydrochemical data (except pH) were log-transformed prior to statistical analyses. The hydrochemical data was also auto-scaled by calculating the standard scores (z scores) and ensuring that all z scores are $<\pm 2.5$. For trace metals with concentrations below their detection limits, one-half of the value of their respective detection limit was substituted and used in statistical analysis. A probability value of $P < 0.05$ was considered as statistically significant in this study.

Results and discussion

The hydrochemical data for groundwater within the basin and their GPS Coordinates is presented in Table 1, while the trace metal levels in groundwater and the GPS Coordinates is presented in Table 2. The statistical summary of the hydrochemical data is presented in Table 3. The Spearman's correlation matrix generated (Table 4) indicate that pH shows low-to-moderate correlation with all major and minor ions (except K and NO_3–N). The Spearman's correlation matrix also shows that HCO_3^- had relatively high correlations with major ions. According to Hounslow (1995), essentially in silicate weathering reactions, bicarbonate is produced, suggesting that HCO_3^- perhaps, originates primarily from silicate weathering reactions in groundwater within the basin. Total dissolved solids (TDS) show strong correlation with, Ca^{2+} ($r = 0.78$; $p < 0.05$), Mg^{2+} ($r = 0.71$; $p < 0.05$), Na^+ ($r = 0.72$; $p < 0.05$), K^+ ($r = 0.62$; $p < 0.05$), Cl^- ($r = 0.74$; $p < 0.05$) and SO_4^{2-} ($r = 0.64$; $p < 0.05$) (Table 4) suggesting that these major ions contributes positively to the total dissolved solids of the groundwater and can be accounted for by a major geochemical process, perhaps aluminosilicate weathering and also originating from the same source (Subba Rao 2002). Correlation analysis of major ions revealed expected process-based relationships between Mg^{2+} and Ca^{2+} ($r = 0.84$; $p < 0.05$), Ca^{2+} and Na^+ ($r = 0.79$; $p < 0.05$), Ca^{2+} and K^+ ($r = 0.65$; $p < 0.05$), Ca^{2+} and Cl^- ($r = 0.84$; $p < 0.05$), Ca^{2+} and SO_4^{2-} ($r = 0.79$; $p < 0.05$), Ca^{2+} and HCO_3^- ($r = 0.73$; $p < 0.05$), Mg^{2+} and Na^+ ($r = 0.87$; $p < 0.05$), Mg^{2+} and K^+ ($r = 0.72$; $p < 0.05$), Mg^{2+} and Cl^- ($r = 0.94$; $p < 0.05$), Mg^{2+} and SO_4^{2-} ($r = 0.93$; $p < 0.05$), Na^+ and K^+ ($r = 0.79$; $p < 0.05$), Na^+ and Cl^- ($r = 0.93$; $p < 0.05$), Na^+ and SO_4^{2-} ($r = 0.91$; $p < 0.05$), K^+ and Cl^- ($r = 0.78$; $p < 0.05$), K^+ and SO_4^{2-} ($r = 0.81$; $p < 0.05$) and Cl^- and SO_4^{2} ($r = 0.92$; $p < 0.05$), derived mainly from the geochemical processes, such as ion-exchange and silicate/aluminosilicate weathering within the aquifer. These process-based relationships between the observed parameters may be due to mineralogical influence which would be explicitly explained by factor loadings during principal component analysis (PCA). The correlation between Cu^{2+} and Zn^{2+} ($r = 0.92$; $p < 0.05$) reveals the possible existence of a process-based (biochemical) relationship between the two metals. Zinc is one of the earliest known trace metal and a common environmental pollutant which is widely distributed in the aquatic environment, while copper is intimately related to the aerobic degradation of organic matter (Das and Nolting 1993). Aerobic degradation of organic matter in groundwater within the basin may, therefore, be responsible for the strong correlation between Cu^{2+} and Zn^{2+}. The correlation matrix also shows the expected strong positive correlation between total hardness (TH) and Ca^{2+} ($r = 0.86$; $p < 0.05$), TH and Mg^{2+} ($r = 0.71$; $p < 0.05$) as calcium and magnesium ions are naturally responsible for hardness in water.

Data analysis using principal component analysis (PCA)

PCA using Varimax with Kaiser normalization has resulted in the extraction of three main principal components which identifies the factors influencing each principal components for the physico-chemical parameters. The three principal components have accounted for approximately 79% of the total variance in the hydrochemical data. Table 6 presents the determined initial principal component and its eigenvalues and per cent of variance contributed in each principal component, while, Table 8 presents the rotated component matrix of the main physico-chemical parameters. The component plot in rotated space is presented in Fig. 2. An eigenvalue gives a measure of the significance of the factor and the factor with the highest eigenvalue as the most significant. Eigenvalues of 1.0 or greater are considered significant (Kim and Mueller 1978). Factor loadings are classified as 'strong', 'moderate' and 'weak' corresponding to absolute loading values of >0.75, 0.75–0.50, and 0.50–0.30, respectively (Liu et al. 2003).

Component 1 explains nearly 51.9% of the total variance (Table 6) and has strong positive loadings (>0.75) for EC, TDS, Mg^{2+}, Ca^{2+}, Na^+, K^+, Cl^- and SO_4^{2-} and a weak positive loading for HCO_3^- (Table 5) suggesting that the

Table 1 Hydrochemical data of groundwater within the Lower Pra Basin and their GPS coordinates

Sample source	BHID	Long	Lat	*T* (°C)	pH	EC	TDS	Turb	Alk	TotH	Ca^{2+}	Mg^{2+}
Assin Nyakomase		5.75724	−1.290630	26.9	4.9	470	276.0	11.9	7.0	38.5	17.1	6.6
Assin Nyakomase		5.75719	−1.290840	27.6	5.3	180	118.1	2.3	13.4	34.7	4.4	6.9
Assin Nyakomase		5.75897	−1.286520	27.1	5.2	70	44.4	2.1	16.7	38.4	2.4	7.3
Brofoyedru Habitat	101 BU3	5.73346	−1.284570	26.3	5.9	120	59.5	1.5	32.2	33.0	5.5	4.5
Akonfude		5.82570	−1.309880	25.7	6.2	290	170.5	1.5	61.5	93.5	22.6	8.2
Akonfude		5.82950	−1.310110	26.2	5.8	500	286.0	7.6	8.6	117.0	21.1	17.0
Assin Breku		5.86801	−1.340940	26.9	6.2	280	173.0	2.0	41.0	85.5	21.3	8.5
Assin Breku (Gyidi)	102 BU3	5.87059	−1.336030	25.6	6.9	320	198.6	3.8	153.0	152.0	38.0	13.6
Assin Breku (SDA)	100 BU3	5.86625	−1.336030	25.7	6.4	140	75.9	1.4	53.1	43.5	15.9	2.0
Techiman No. 1	396 BU3	5.80432	−1.367920	26.7	5.3	60	33.1	1.3	20.8	12.9	3.6	2.4
Kwame Ankra	411 BU3	5.81542	−1.381990	26.5	5.8	143	80.7	1.6	35.9	35.0	13.6	1.6
Ninkyiso		5.82117	−1.399120	28.2	5.2	210	119.0	1.4	13.6	34.5	7.0	4.3
Sabina	380 BU1	5.86974	−1.271720	29.2	6.9	270	141.6	2.9	87.0	82.5	21.2	6.6
Ayitey	094 BU3	5.88353	−1.255840	28.5	7.3	200	118.6	1.5	54.2	61.5	14.6	4.5
Nkrafo	098 BU3	5.87809	−1.233640	28.1	7.9	360	216.0	4.0	161.0	134.0	38.3	12.6
Nkrafo	096 BU3	5.88087	−1.238620	29.3	6.5	180	260.0	90.8	8.7	58.5	16.6	4.0
Obirikwaku	099 BU3	5.91571	−1.236610	29.1	6.3	260	149.0	1.4	113.0	99.0	31.0	5.5
Odumase Camp	405 BU2	5.82454	−1.191470	30.5	6.0	150	83.3	44.3	19.1	23.0	8.2	5.1
Obobakokrowa		5.82490	−1.177680	28.7	6.3	310	198.1	14.1	139.6	145.5	47.5	7.2
Obobakokrowa	246 J BU1	5.83276	−1.176530	28.3	5.7	290	163.5	2.0	29.5	83.5	15.4	11.7
Odumase Camp	407 BU2	5.82181	−1.194190	29.1	6.1	310	176.9	15.2	61.0	74.5	14.7	9.9
Dwedaama		5.90170	−1.204960	28.0	6.5	240	193.5	13.0	153.0	155.0	42.4	14.6
Dwedaama		5.80159	−1.205750	28.2	5.8	90	52.8	1.9	27.8	45.0	15.6	2.8
Amoakokrom	337 BU3	5.85972	−1.256110	28.8	5.8	320	131.0	2.9	47	34.0	12.2	3.8
Worakese Habitat	097 BU3	5.76443	−1.131540	27.2	5.6	80	56.2	1.4	27.1	21.1	3.4	3
Antoabasa		5.77196	−1.468780	30.4	6.1	170	98.8	1.6	50.1	51.5	10.1	5.6
Antoabasa		5.7702	−1.469480	30.2	5.9	220	137.0	12.0	46.4	47.7	11.7	4.7
Bediadua		5.77278	−1.497220	29.2	5.9	220	83.5	2.4	98.0	43.2	17.2	6.1

Sample source	Na^{+}	K^{+}	Cl^{-}	HCO_3^{-}	NO_3N	PO_4P	SO_4^{2-}	SiO_2	F^{-}	NH_4–N	E.Bal	CBE (%)
Assin Nyakomase	57.5	50	64.6	105.8	1.550	0.160	55.6	11.6	<0.005	<0.001	0.37	4.10
Assin Nyakomase	28.3	9.2	18.1	68.6	0.941	0.351	18.1	26.7	<0.005	<0.001	0.18	3.72
Assin Nyakomase	19.9	6.4	13.1	36.3	1.853	0.643	18.7	6.8	<0.005	<0.001	−0.05	−1.98
Brofoyedru Habitat	18.2	7.1	10.4	47.4	1.200	0.570	17.9	7.9	<0.005	<0.001	−0.18	−4.68
Akonfude	24.0	15.0	57.6	95.7	0.300	0.260	31.2	35.0	<0.005	<0.001	−0.18	−2.58
Akonfude	34.0	5.4	54.7	96.8	0.650	0.320	25.3	24.3	<0.005	<0.001	0.28	3.64
Assin Breku	25.3	6.4	42.8	99.8	0.690	0.410	6.2	32.9	<0.005	<0.001	0.04	0.64
Assin Breku (Gyidi)	26.0	5.0	9.0	187.8	0.070	0.210	43.7	31.3	<0.005	<0.001	−0.12	−1.43
Assin Breku (SDA)	14.1	3.5	18.8	64.4	0.360	0.380	4.0	5.0	<0.005	<0.001	−0.12	−3.70
Techiman No. 1	9.5	3.4	6.5	25.9	0.450	0.400	13.0	1.4	<0.005	<0.001	0.02	1.22
Kwame Ankra	18.6	5.3	14.9	56.9	3.300	0.260	9.3	35.2	<0.005	<0.001	0.05	1.72
Ninkyiso	26.5	5.7	21.8	66.1	0.660	0.250	12.6	18.8	<0.005	<0.001	−0.14	−3.21
Sabina	25.5	5.7	16.0	109.9	0.280	0.200	18.8	32.8	<0.005	<0.001	0.11	2.66
Ayitey	17.8	6.9	21.9	67.8	0.570	0.180	8.9	1.6	<0.005	<0.001	0.25	4.65
Nkrafo	34.0	9.3	18.9	196	0.070	0.060	4.7	1.4	<0.005	<0.001	0.17	4.12
Nkrafo	12.9	4.8	12.9	64.5	1.490	0.030	10.9	23.0	<0.005	<0.001	0.40	4.86
Obirikwaku	17.7	5.9	11.9	136.8	0.200	0.180	18.4	33.7	<0.005	<0.001	0.05	1.46
Odumase Camp	16.2	3.3	11.4	33.4	0.180	0.090	11.8	5.0	<0.005	<0.001	0.07	1.19
Obobakokrowa	18.8	3.4	20.4	169.9	0.160	0.160	6.6	4.1	<0.005	<0.001	0.12	5.02

Table 1 continued

Sample source	Na^+	K^+	Cl^-	HCO_3^-	NO_3N	PO_4P	SO_4^{2-}	SiO_2	F^-	NH_4–N	E.Bal	CBE (%)
Obobakokrowa	34.5	2.7	36.2	92.7	0.640	0.200	14.1	34.3	<0.005	<0.001	0.27	3.75
Odumase Camp	41.5	4.6	47.8	85.8	0.540	0.170	31.7	18.2	<0.005	<0.001	0.20	3.25
Dwedaama	22.0	7.4	7.0	195.3	0.060	0.560	35.0	9.6	<0.005	<0.001	0.04	0.52
Dwedaama	9.4	3.1	12.4	35.7	0.280	0.250	14.0	18.0	<0.005	<0.001	0.24	2.83
Amoakokrom	30.6	5.2	34.8	54.7	0.070	1.200	24.1	24.7	<0.005	<0.001	0.13	5.04
Worakese Habitat	14.8	6.6	15.4	31.8	1.880	0.540	7.4	15.9	<0.005	<0.001	0.07	2.96
Antoabasa	25.0	4.5	19	55.6	0.620	0.490	31.8	15.4	<0.005	<0.001	0.00	0.10
Antoabasa	35.0	4.6	32.3	65.1	0.540	0.270	21.9	22.0	<0.005	<0.001	−0.10	−2.13
Bediadua	28.2	1.5	8.1	119.2	0.061	0.480	18.3	28.2	<0.005	<0.001	0.13	2.58

Sample source	BHID	Long	Lat	T°C	pH	EC	TDS	Turb	Alk	TotH	Ca^{2+}	Mg^{2+}
Anum	086 BU3	5.78219	−1.502240	28.8	6.5	270	158.0	8.8	114.0	93.0	24.0	7.5
Kyeikurom	090 BU3	5.82504	−1.522420	28.3	6.0	150	87.1	1.2	55.1	33.1	9.0	2.5
Adukurom	088 BU3	5.82278	−1.524440	31.6	5.6	140	79.6	1.4	43.6	61.2	9.0	9.6
Nsuekyir	219 BU1	5.68667	−1.497220	27.1	5.9	170	100.4	13.7	54.8	87.5	15.7	11.3
Subriso		5.82474	−1.547990	27.0	6.0	240	107.5	2.0	104.0	57.5	13.1	12.9
Danyiase Domeabra	092 BU3	5.74806	−1.538060	26.5	5.9	220	118.5	1.8	81.9	65.5	19.4	5.5
Anyinase Ankase	030 BU3	5.59446	−1.602790	28.0	5.6	100	58.4	1.5	37.0	37.0	8.5	4.1
Gromsa	032 BU3	5.58991	−1.606070	28.6	6.0	190	119.0	1.8	57.1	220.0	32.9	3.5
Somnyamekodur	048D033 BU3	5.66046	−1.583760	30.7	6.4	710	440.0	6.0	139.0	59.5	14.9	5.5
Somnyamekordur		5.66046	−1.583760	29.3	6.6	824	453.0	3.6	228.0	226.0	84.2	3.8
Twifo Agona	263 BU2	5.74595	−1.503980	29.8	6.3	190	110.0	4.8	77.7	53.0	18.3	10
Nyamebekyere	339 BU3	5.80139	−1.721390	29.2	6.0	170	85.4	1.5	53.0	25.5	9.4	3.5
Jerusalem	0502B1/6/097-01	5.81667	−1.717500	28.8	5.9	80	43.2	1.8	25.6	8.3	2.6	2.4
Akwa Yaw		5.44157	−1.465800	26.8	6.1	130	105.0	4.7	124.0	64.0	21.0	14.1
Twifo Mampong		5.52016	−1.554490	26.8	5.3	279	156.0	195	30	68.0	10.4	10.20
Twifo Mampong		5.52359	−1.556810	27.4	6.3	1140	627.0	153	106	324.0	57.7	43.70
Atu Kurom		5.63657	−1.678500	29.5	5.6	350	159.0	18.0	209.5	110.0	32.5	17
Subreso	048D035 BU3	5.65596	−1.676760	28.1	6.1	250	63.1	2.6	67.5	40.2	17.1	10.8
Breman	260 BU2	5.70878	−1.602770	28.9	6.9	310	222.0	80.3	155.6	92.5	29.1	21.8
Breman		5.70720	−1.602610	28.5	6.4	240	114.0	2.8	125.0	64.0	26.0	16.3
Zion Camp	014 BU3	5.87217	−1.646020	29.9	6.6	1601	674.0	4.4	204.0	320.0	155.0	109
Mampong	22/D/73-1	5.111470	−1.731740	27.2	6.1	800	453.0	3.9	64.6	215.0	42.7	30.2
Essamang		5.05042	−1.679790	26.4	5.3	60	36.3	4.6	18.5	18.5	5.7	1.3
Mamponso	24/B/85-1	5.42906	−1.630020	26.7	5.8	110	57.8	1.4	26.6	23.4	15.7	4.0
Sienchem	24/B/32-1	5.47123	−1.650530	25.3	5.7	560	380.0	1.2	37.1	137.0	31.1	13.1
Sienchem	24/B/32-2	5.47246	−1.651560	25.9	5.8	230	120.0	1.3	31.2	39.5	13.5	1.7

Sample source	Na^+	K^+	Cl^-	HCO_3^-	NO_3N	PO_4P	SO_4^{2-}	SiO_2	F^-	NH_4–N	E.Bal	CBE (%)
Anum	29.7	6.2	22.1	140	0.150	0.340	10.3	16.8	<0.005	<0.001	0.10	1.62
Kyeikurom	20.0	3.1	10.1	64.2	0.200	0.340	16.7	20.4	<0.005	<0.001	−0.13	−3.90
Adukurom	15.8	3.6	17.4	72.2	0.410	0.430	3.6	12.9	<0.005	<0.001	0.03	0.65
Nsuekyir	15.6	5.3	23.4	69.3	0.720	0.430	22.2	16.1	<0.005	<0.001	−0.16	−2.94
Subriso	20.7	5.5	13.4	132	0.055	0.100	24.2	30.5	<0.005	<0.001	0.20	4.28
Danyiase Domeabra	18.9	5.4	11.4	107.5	0.070	0.670	22.2	18.1	<0.005	<0.001	0.07	1.65
Anyinase Ankase	11.7	1.7	6.3	44.7	0.370	0.740	9.9	9.2	0.187	<0.001	0.12	1.93
Gromsa	14.3	2.5	30.9	69.8	0.440	1.410	23.8	23.0	<0.005	<0.001	−0.17	−3.02
Somnyamekodur	67.5	3.9	73	144.8	0.320	2.610	13.6	17.4	<0.005	<0.001	0.31	5.19
Somnyamekordur	42.3	12.3	81.4	278.2	0.255	0.309	10.4	27.8	<0.005	<0.001	0.10	4.05

Table 1 continued

Sample source	Na^+	K^+	Cl^-	HCO_3^-	NO_3N	PO_4P	SO_4^{2-}	SiO_2	F^-	NH_4–N	E.Bal	CBE (%)
Twifo Agona	14.1	8	10.1	93.7	0.140	1.990	22.6	18.2	<0.005	<0.001	0.07	1.26
Nyamebekyere	17.6	5.2	19	64.4	0.560	1.900	3.6	16.2	0.181	<0.001	−0.54	−4.95
Jerusalem	10.0	5.4	7.1	28.3	0.360	3.080	7.5	13.1	<0.005	<0.001	−0.18	−2.54
Akwa Yaw	27.2	2.5	7.7	150.3	0.488	0.161	23.8	23.7	0.193	<0.001	−0.54	−5.14
Twifo Mampong	28.0	23	35.7	36.6	0.691	0.669	77.8	31.7	<0.005	<0.001	−0.07	−1.15
Twifo Mampong	23.6	20	174	129.3	0.36	0.558	76.8	17.8	<0.005	<0.001	−2.06	−3.47
Atu Kurom	37.9	16	10.1	250.4	0.393	0.429	58.7	28.5	<0.005	<0.001	−0.44	−4.99
Subreso	28.6	2.9	9.1	82.1	0.285	0.156	62.1	24.3	<0.005	<0.001	−0.41	−2.96
Breman	41.3	13	37.7	190.4	1.419	0.271	75.7	22.9	<0.005	<0.001	0.24	5.09
Breman	21.9	3.4	13.9	150.8	0.280	0.268	44.9	32.2	<0.005	<0.001	0.00	0.08
Zion Camp	226.0	65	693	241.6	0.457	0.362	353	25.5	<0.005	<0.001	0.02	1.32
Mampong	63.5	9.5	163	82.4	3.045	0.437	75.9	10.6	<0.005	<0.001	0.15	1.01
Essamang	7.4	0.6	5.7	28.5	0.554	0.502	1.6	18.0	<0.005	<0.001	0.06	4.18
Mamponso	13.5	2.5	11.1	32.5	4.190	0.210	32.2	9.1	<0.005	<0.001	0.18	5.38
Sienchem	62.5	16	75.6	115.2	3.474	0.306	91	21.6	<0.005	<0.001	−0.21	−1.82
Sienchem	18.2	15	23.2	36.9	1.690	0.342	31.9	11.1	<0.005	<0.001	0.04	0.97

All parameters are in mg/L, except, temperature (°C), pH (pH units), conductivity (μS/cm)

BHID borehole identification number, *Temp* temperature, *Cond* conductivity, *TotH* total hardness, *E.Bal* electrical balance, *CBE* charge balance error

major ions contribute positively to the total dissolved solids of the groundwater and can be accounted for by major geochemical processes within the aquifer. By their definitions, TDS is the total dissolved solids, while, EC is the total ions in solution. In general, a plot of TDS against EC shows a linear relationship with slope (m), and TDS − conductivity factor (r^2). The general equation for this linear graph can be represented as $KA = S$, where, K is the EC (μS/cm), S is the TDS (mg/L), and A is a constant which defines whether a particular water type is high in HCO_3^-, SO_4^{2-} or Cl^- (Clark and Fritz 1997). Tay et al. (2014) reported that, 72.4% of groundwater within the basin had $A = 0.55$ and therefore, suggest that groundwater within the basin is high in HCO_3^-, and probably suggest the role of silicate weathering by carbon-dioxide charged water during water–rock interaction in the aquifers. This is also consistent with the TDS-EC correlation in the Spearman's correlation table (Table 4), where, TDS show strong correlation with EC ($r = 0.96$; $p < 0.05$). Thus, the strong positive loadings of the major ions together with EC and TDS in Component 1 are expected and suggest their contribution to major geochemical processes through mineralogical influence.

Component 2 explains approximately 17.5% of the total variance (Table 6) and has strong positive loadings for pH, SiO_2 and HCO_3^- and weak negative loadings for PO_4–P and NO_3–N (Table 5) reflecting a common source, clearly, silicate/aluminosilicate weathering by carbon-dioxide charged water. The strong positive loadings for SiO_2, HCO_3^- and pH in the groundwater, suggests sorption of silica by clay minerals (Siever and Woodward 1973). This is consistent with the results by Tay et al. (2014) that, dissolved silica in groundwater within the Lower Pra Basin originates from the chemical breakdown of silicates during weathering processes.

Component 3 explains approximately 9.5% of the total variance (Table 6) and has moderate positive loading for NO_3–N and moderate negative loading for PO_4–P (Table 5). Component 3 though reflects a common source of anthropogenic origin (possibly pollution from human induced activities, such as inorganic fertilizer), it shows how NO_3–N and PO_4–P correlates significantly with each other, i.e., where, NO_3–N concentration is high, PO_4–P concentration is low. The economic activity within the basin is primarily, farming, where foodstuffs, such as yam, plantain, banana, vegetables, fruits, and cash crops, such as cocoa, oil palm, and coffee, are grown. Land degradation as a result of poor farming practices where indiscriminate use of nitrogen and phosphorus based fertilizers are widespread and in some cases agrochemicals are used, are some of the human induced activities which are most likely to have anthropogenic impact on the water resources within the basin.

The results of the PCA for the physico-chemical and trace metals data using Varimax with Kaiser normalization rotation are presented in Tables 7 and 8. Five principal components accounting for 85.2% of the total variance have been extracted on the basis of the eigenvalues >1 (Table 8). The first three principal components explain 48.09, 14.62 and 8.47% of the total variance, respectively.

Table 2 Trace metal levels in groundwater within the Lower Pra Basin and their GPS Coordinates

Sample source	BHID	Longitude	Latitude	Cu	Mn	Zn	Cd	Pb	Fe	Al	As	Hg	Se
Assin Nyakomase		5.75724	−1.29063	0.053	0.092	<0.005	<0.002	0.062	0.526	0.226	<0.050	5.450	10.30
Assin Nyakomase		5.75719	−1.29084	<0.020	0.008	<0.005	<0.002	0.059	0.160	<0.010	<0.050	5.910	5.400
Assin Nyakomase		5.75897	−1.28652	<0.020	0.027	<0.005	<0.002	0.022	0.576	0.251	<0.050	4.510	<0.010
Brofoyedru Habitat	101 BU3	5.73346	−1.28457	0.020	0.013	<0.005	<0.002	0.054	0.075	0.067	<0.050	8.270	<0.010
Akonfude		5.82570	−1.30988	0.020	0.058	<0.005	<0.002	0.026	0.465	0.061	<0.050	7.300	<0.010
Akonfude		5.82950	−1.31011	<0.020	0.035	0.0070	<0.002	0.049	0.714	0.055	<0.050	4.270	<0.010
Assin Breku		5.86801	−1.34094	<0.020	0.050	<0.005	<0.002	0.055	0.492	0.237	<0.050	4.120	<0.010
Assin Breku (Gyidi)	102 BU3	5.87059	−1.33603	<0.020	0.400	<0.005	<0.002	0.059	<0.010	<0.010	<0.050	2.720	<0.010
Assin Breku (SDA)	100 BU3	5.86625	−1.33603	<0.021	<0.005	<0.005	<0.002	<0.005	0.156	<0.010	<0.050	0.960	<0.010
Techiman No. 1	396 BU3	5.80432	−1.36792	0.083	0.036	0.0100	<0.002	0.039	0.087	0.010	<0.050	1.540	<0.010
Kwame Ankra	411 BU3	5.81542	−1.38199	<0.020	0.043	<0.005	<0.002	0.040	0.044	0.132	<0.050	1.110	<0.010
Ninkyiso		5.82117	−1.39912	<0.020	0.041	<0.005	<0.002	0.036	0.042	<0.010	<0.050	1.360	<0.010
Sabina	380 BU1	5.86974	−1.27172	<0.020	<0.005	<0.005	<0.002	<0.005	0.042	0.019	<0.050	0.760	<0.010
Ayitey	094 BU3	5.88353	−1.25584	<0.020	0.067	<0.005	<0.002	0.014	0.186	<0.010	<0.050	8.180	<0.010
Nkrafo	098 BU3	5.87809	−1.23364	<0.020	0.083	<0.005	<0.002	<0.005	0.068	<0.010	<0.050	8.250	<0.010
Nkrafo	096 BU3	5.88087	−1.23862	<0.020	0.141	<0.005	<0.002	<0.005	0.040	<0.010	<0.050	3.690	<0.010
Obirikwaku	099 BU3	5.91571	−1.23661	0.079	0.258	0.0660	<0.002	0.018	0.088	<0.010	<0.050	5.130	<0.010
Odumase Camp	405 BU2	5.82454	−1.19147	<0.020	0.044	<0.005	<0.002	0.048	2.130	0.112	<0.050	2.380	<0.010
Obobakokrowa		5.82490	−1.17768	<0.020	0.096	<0.005	<0.002	0.015	0.249	<0.010	<0.050	0.530	<0.010
Obobakokrowa	246 J BU1	5.83276	−1.17653	<0.020	<0.005	<0.005	<0.002	0.048	0.068	0.081	<0.050	1.550	0.990
Odumase Camp	407 BU2	5.82181	−1.19419	<0.020	<0.005	0.0430	<0.002	0.005	0.047	0.195	0.1700	2.000	0.350
Dwedaama		5.90170	−1.20496	<0.020	<0.005	<0.005	<0.002	0.010	0.106	<0.010	<0.050	0.680	1.410
Dwedaama		5.80159	−1.20575	<0.020	0.009	<0.005	<0.002	<0.005	0.409	0.727	<0.050	3.810	<0.010
Amoakokrom	337 BU3	5.85972	−1.25611	<0.020	0.087	<0.005	<0.002	<0.005	0.121	0.119	0.1300	3.690	0.200
Worakese Habitat	097 BU3	5.76443	−1.13154	<0.020	<0.005	<0.005	<0.002	<0.005	0.108	0.296	<0.050	4.020	0.200
Antoabasa		5.77196	−1.46878	<0.020	<0.005	0.0980	0.0030	<0.005	<0.010	0.182	0.1300	1.840	0.350
Antoabasa		5.77018	−1.46948	<0.020	0.053	<0.005	<0.002	<0.005	0.476	0.179	0.2500	3.860	<0.010
Bediadua		5.77278	−1.49722	<0.020	0.071	<0.005	<0.002	<0.005	0.178	0.176	0.1600	5.740	<0.010
Anum	086 BU3	5.78219	−1.50224	<0.020	0.027	<0.005	<0.002	<0.005	0.038	<0.010	0.0500	6.040	<0.010
Kyeikurom	090 BU3	5.82504	−1.52242	<0.020	0.057	<0.005	<0.002	<0.005	0.368	0.162	0.1500	0.590	1.160
Adukurom	088 BU3	5.82278	−1.52444	<0.020	<0.005	<0.005	<0.002	<0.005	0.045	0.399	<0.05	1.060	<0.010
Nsuekyir	219 BU1	5.68667	−1.49722	<0.020	<0.005	<0.005	<0.002	<0.005	0.101	0.157	0.1000	2.440	<0.010
Subriso		5.82474	−1.54799	<0.020	0.006	<0.005	<0.002	0.008	0.101	<0.010	<0.05	2.280	<0.010
Danyiase Domeabra	092 BU3	5.74806	−1.53806	<0.020	0.008	<0.005	<0.002	<0.005	0.924	<0.010	<0.05	3.930	<0.010
Anyinase Ankase	030 BU3	5.59446	−1.60279	<0.020	<0.005	<0.006	<0.002	<0.005	<0.010	<0.011	<0.05	1.940	<0.010
Gromsa	032 BU3	5.58991	−1.60607	0.020	0.093	<0.005	<0.002	<0.005	0.178	0.694	0.340	3.950	<0.010
Somnyamekodur	048D033 BU3	5.66046	−1.58376	0.020	0.021	0.030	<0.002	<0.005	0.081	0.528	0.090	10.09	<0.010
Somnyamekordur		5.66046	−1.58376	<0.020	0.021	<0.005	<0.002	<0.005	0.078	0.017	0.060	5.720	<0.010
Twifo Agona	263 BU2	5.74595	−1.50398	<0.020	0.053	<0.005	<0.002	<0.005	0.181	<0.010	0.090	2.980	<0.010
Nyamebekyere	339 BU3	5.80139	−1.72139	<0.020	0.047	<0.005	<0.002	<0.005	0.514	0.386	<0.05	7.380	<0.010
Jerusalem	0502B1/6/09701	5.81667	−1.71750	<0.020	0.037	<0.005	<0.002	<0.005	0.220	<0.010	0.180	4.110	<0.010
Akwa Yaw		5.44157	−1.46580	<0.020	0.069	<0.005	<0.002	<0.005	0.103	0.285	<0.05	3.300	<0.010
Twifo Mampong		5.52016	−1.55449	<0.020	0.089	<0.005	<0.002	<0.005	0.441	0.359	<0.05	3.330	<0.010

Table 2 continued

Sample source	BHID	Longitude	Latitude	Cu	Mn	Zn	Cd	Pb	Fe	Al	As	Hg	Se
Twifo Mampong		5.52359	−1.55681	<0.020	0.073	<0.005	<0.002	0.007	0.150	<0.010	0.430	<0.010	<0.010
Atu Kurom		5.63657	−1.67850	<0.020	0.261	0.041	<0.002	<0.005	0.186	0.043	19.10	1.530	<0.010
Subreso	048D035 BU3	5.65596	−1.67676	<0.020	0.103	<0.005	<0.002	<0.005	<0.010	0.123	3.010	1.540	<0.010
Breman	260 BU2	5.70878	−1.60277	<0.020	0.014	<0.005	<0.002	<0.005	0.113	<0.010	1.820	0.890	<0.010
Breman		5.70720	−1.60261	<0.020	<0.005	<0.005	<0.002	0.024	0.103	<0.010	1.590	5.120	<0.010
Zion Camp	014 BU3	5.87217	−1.64602	0.023	0.185	<0.005	<0.002	0.021	0.108	<0.010	1.520	4.500	<0.010
Mampong	22/D/73-1	5.11147	−1.73174	<0.020	0.682	0.008	<0.002	0.026	0.105	<0.010	1.930	4.670	<0.010
Essamang		5.05042	−1.67979	<0.020	0.015	<0.005	<0.002	<0.005	0.068	0.162	2.110	<0.010	<0.010
Mamponso	24/B/85-1	5.42906	−1.63002	<0.020	0.044	<0.005	<0.002	0.031	0.170	0.176	2.310	<0.010	<0.010
Sienchem	24/B/32-1	5.47123	−1.65053	0.395	0.752	0.314	<0.002	<0.005	0.108	0.072	1.160	<0.010	<0.010
Sienchem	24/B/32-2	5.47246	−1.65156	<0.020	2.280	<0.005	<0.002	<0.005	0.125	<0.010	0.900	<0.010	<0.010

All parameters are in mg/L

Table 3 Summary statistics of hydrochemical data for groundwater within the Lower Pra Basin

Parameter	Min	Max	Mean	Median	SD
Temp	25.3	31.6	28.0	28.2	1.5
pH	4.9	6.9	6.0	6.0	0.5
EC	60	1601	314.8	225.0	273.5
TDS	33.1	674	173.7	119.0	138.9
TotH	8.3	324	84.9	60.4	69.7
Ca^{2+}	2.4	155	24.4	15.8	23.7
Mg^{2+}	1.3	109	12.1	6.6	15.5
Na^{+}	7.4	226	32.4	22.8	30.5
K^{+}	0.6	65	9.4	5.4	10.8
Cl^{-}	5.7	693	52.5	18.5	96.3
HCO_3^{-}	25.9	278.2	100.1	82.3	60.9
NO_3–N	0.055	4.19	0.8	0.5	0.9
SO_4^{2-}	1.6	353.2	37.2	18.8	49.7
SiO_2	1.4	35.2	19.3	18.2	9.6
PO_4–P	0.03	3.08	0.561	0.863	0.60
Cu	<0.020	0.395	0.079	0.023	0.12
Mn	<0.005	2.280	0.155	0.053	0.37
Zn	<0.005	0.314	0.069	0.041	0.097
Cd	<0.002	0.003	–	–	–
Pb	<0.005	0.062	0.032	0.029	0.019
Fe	<0.010	2.130	0.245	0.117	0.336
Al	<0.010	0.727	0.209	0.169	0.179
As	<0.05	19.100	1.574	0.295	3.838
Hg	<0.010	10.090	3.694	3.690	2.350
Se	<0.010	10.300	2.262	0.990	3.425

The fourth and fifth principal components are considerably less important, explaining only 7.02 and 6.94% of the total variance, respectively. Thus, the first three principal components as extracted in Table 7, accounting for a large proportion (71.2%) of total variance in the hydrochemical data are considered. Table 7 presents the determined initial principal component and its eigenvalues and per cent of variance contributed in each principal component, while, Table 8 presents the rotated component matrix of the main physico-chemical and trace metal parameters. Component 1 explains nearly 48.09% of the total variance (Table 8) and has strong positive loadings (>0.75) for the major ions (EC, TDS, Mg^{2+}, Ca^{2+}, Na^{+}, K^{+}, Cl^{-} and SO_4^{2-}), a moderate positive loading for HCO_3^{-} and a weak positive

Table 4 Spearman's correlation matrix for groundwater within the Lower Pra Basin

	pH	EC	TDS	TH	Ca	Mg	Na	K	Cl	HCO_3	NO_3N	PO_4P
pH	1.00											
EC	0.27	1.00										
TDS	0.31	**0.96**	1.00									
TH	0.40	**0.82**	**0.83**	1.00								
Ca	0.42	**0.85**	**0.78**	**0.86**	1.00							
Mg	0.23	**0.83**	**0.71**	**0.71**	**0.84**	1.00						
Na	0.16	**0.82**	**0.72**	0.55	**0.79**	**0.87**	1.00					
K	−0.03	**0.70**	**0.62**	0.47	**0.65**	**0.72**	**0.79**	1.00				
Cl	0.16	**0.85**	**0.74**	**0.66**	**0.84**	**0.94**	**0.93**	**0.78**	1.00			
HCO_3	0.52	0.58	0.58	**0.64**	**0.73**	0.48	0.48	0.36	0.37	1.00		
NO_3N	−0.26	0.01	0.08	−0.07	−0.09	−0.02	0.06	0.10	0.04	−0.27	1.00	
PO_4P	−0.07	−0.01	−0.02	−0.12	−0.14	−0.10	−0.04	−0.09	−0.03	−0.16	−0.15	1.00
SO_4	0.11	**0.76**	**0.64**	0.59	**0.79**	**0.93**	**0.91**	**0.81**	**0.92**	0.40	0.10	−0.10
SiO_2	−0.02	0.16	0.14	0.15	0.16	0.13	0.15	0.08	0.10	0.29	−0.10	−0.10
Cu	−0.11	−0.03	−0.04	−0.10	−0.05	−0.10	−0.05	0.12	−0.03	−0.14	0.13	−0.06
Mn	−0.03	−0.03	−0.03	−0.05	−0.05	−0.09	−0.09	−0.01	−0.07	−0.08	0.06	−0.08
Zn	−0.03	−0.04	−0.06	−0.08	−0.04	−0.10	−0.06	0.04	−0.05	−0.12	0.09	−0.08
Cd	0.02	−0.06	−0.07	−0.06	−0.07	−0.04	−0.02	−0.05	−0.03	−0.10	−0.02	−0.01
Pb	−0.28	0.05	0.06	−0.03	−0.03	0.04	0.12	0.21	0.07	−0.06	0.17	−0.25
Fe	−0.18	−0.05	−0.06	−0.13	−0.14	−0.05	−0.09	−0.01	−0.04	−0.23	−0.12	0.00
Al	−0.12	0.16	0.20	0.01	−0.03	−0.09	0.01	0.03	0.01	−0.04	0.04	0.30
As	0.03	0.04	−0.04	−0.04	0.04	0.09	0.09	−0.01	0.03	0.01	0.06	−0.11
Hg	0.22	0.17	0.16	0.07	0.14	0.03	0.11	0.16	0.14	0.09	−0.22	0.18
Se	−0.35	0.04	0.06	−0.11	−0.08	−0.05	0.10	0.46	0.00	0.00	0.10	−0.10

	SO_4	SiO_2	Cu	Mn	Zn	Cd	Pb	Fe	Al	As	Hg	Se
pH												
EC												
TDS												
TH												
Ca												
Mg												
Na												
K												
Cl												
HCO_3												
NO_3N												
PO_4P												
SO_4	1.00											
SiO_2	0.17	1.00										
Cu	−0.01	−0.14	1.00									
Mn	−0.03	0.00	0.64	1.00								
Zn	−0.01	−0.08	**0.92**	0.62	1.00							
Cd	0.00	−0.06	−0.03	−0.08	0.26	1.00						
Pb	0.05	0.09	−0.03	0.06	−0.14	−0.10	1.00					
Fe	−0.10	−0.25	−0.06	−0.10	−0.10	−0.10	0.26	1.00				
Al	−0.09	0.02	−0.06	−0.16	−0.03	0.04	−0.19	0.11	1.00			
As	0.20	0.08	0.01	0.24	0.11	−0.03	−0.12	−0.07	−0.09	1.00		
Hg	−0.03	−0.04	−0.17	−0.07	−0.18	−0.09	0.12	0.08	0.16	−0.17	1.00	
Se	0.03	−0.06	0.05	−0.05	−0.05	0.00	0.44	0.08	0.02	−0.06	0.12	1.00

Bold values indicate high correlation (at significant level of $P < 0.05$) and shows evidence of observed water composition

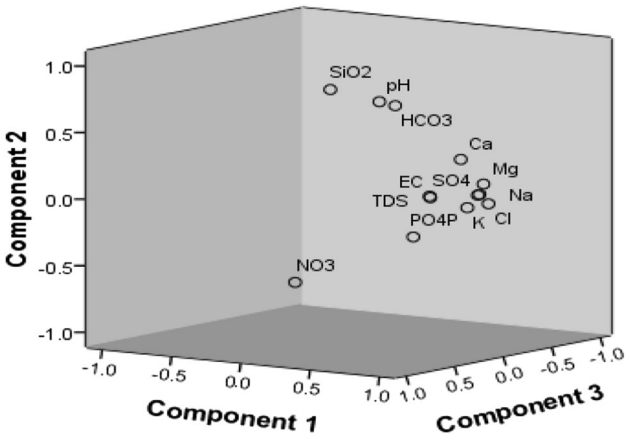

Fig. 2 Component plot in rotated space for groundwater within the Basin

loading for pH (Table 7) suggesting that, the major ions contribute positively to the total dissolved solids of the groundwater and can be accounted for by major geochemical processes within the aquifer.

Component 2 explains approximately 14.67% of the total variance (Table 8) and has moderate negative loadings for HCO_3^-, pH; moderate positive loadings for NO_3–N and Mn and a strong negative loading for SiO_2 (Table 7) reflecting a natural source (silicate/aluminosilicate weathering by carbon-dioxide charged water) and anthropogenic source (use of inorganic fertilizer in agricultural activities). Component 3 explains approximately 8.47% of the total variance (Table 8) and has moderate positive loadings for Pb and Fe; moderate negative loadings for Cu and Zn and weak positive loadings for Hg and Se (Table 7). Component 3 though, reflects a common source of trace metal mobilization, it shows how Pb, Fe, Hg and Se and; Cu and Zn correlates, i.e. where Pb, Fe, Hg and Se concentration is high, Cu and Zn concentration is low. This PCA results is consistent with results from the Spearman's Correlation matrix that, correlation between Cu^{2+} and Zn^{2+} ($r = 0.92$; $p < 0.05$), reveals the possible existence of a process-based relationship between the two metals.

The loadings and score plots of the first two PCs which explain 62.75% of variance is presented in Fig. 3. Figure 3 shows grouping and relationship between the variables. The major, EC and TDS are visible in the first and second quadrants and have been shown to group together indicating their close relations. HCO_3^-, pH and SiO_2 have also been shown to group together indicating their relationship and significance in silicate weathering within the basin, while, trace metals have also grouped together reflecting a common source. This grouping pattern shows the strength of the mutual relation among the hydrochemical variables.

Thus, from the PCA, it can be deduced that, Component 1 delineates the main natural processes (water–soil–rock interactions) through which groundwater within the basin acquires its chemical characteristics, Component 2 delineates the incongruent dissolution of silicate/aluminosilicates, while, Component 3 delineates the prevalence of pollution principally from agricultural input as well as trace metal mobilization in groundwater within the basin.

Hydrogeochemical processes influencing groundwater within the Lower Pra Basin

According to Tay et al. (2014), the major processes responsible for chemical evolution of groundwater within

Table 5 Component matrix of the main physico-chemical parameters

Chemical parameter	Component		
	1	2	3
Na^+	**0.969**	0.092	0.038
Cl^-	**0.960**	0.005	−0.068
Mg^{2+}	**0.936**	0.152	−0.052
SO_4^{2-}	**0.923**	0.073	−0.012
K^+	**0.870**	−0.021	0.022
Ca^{2+}	**0.864**	0.349	0.079
TDS	**0.832**	0.097	0.348
EC	**0.831**	0.109	0.354
SiO_2	−0.147	**0.757**	−0.021
pH	0.267	**0.720**	0.065
HCO_3^-	0.413	**0.712**	0.111
NO_3–N	0.109	−0.560	**0.708**
PO_4–P	−0.008	−0.430	**−0.677**

Extraction method: principal component analysis using Varimax with Kaiser normalization

Values in bold represent 'strongly loaded' (>0.75) or 'moderately loaded' (0.5–0.75) or 'weakly loaded' (<0.5)

Table 6 Total variance explained

Component	Initial eigen values			Extraction sums of squared loadings			Rotation sums of squared loadings		
	Total	% of Variance	Cumulative %	Total	% of Variance	Cumulative %	Total	% of Variance	Cumulative %
1	7.090	54.538	54.538	7.090	54.538	54.538	6.752	51.941	51.941
2	2.038	15.677	70.214	2.038	15.677	70.214	2.278	17.525	69.467
3	1.141	8.778	78.992	1.141	8.778	78.992	1.238	9.526	78.992
4	0.804	6.186	85.179						
5	0.697	5.363	90.541						
6	0.390	2.997	93.538						
7	0.328	2.521	96.059						
8	0.271	2.086	98.145						
9	0.134	1.034	99.179						
10	0.059	0.454	99.633						
11	0.036	0.277	99.910						
12	0.008	0.060	99.970						
13	0.004	0.030	100.000						

Extraction method: principal component analysis

Table 7 Component matrix of hydrochemical data for groundwater within the Lower Pra Basin

	Component		
Chemical parameter	1	2	3
pH	0.349	**−0.653**	0.088
EC	**0.888**	0.054	−0.039
TDS	**0.886**	0.063	−0.041
Ca^{2+}	**0.898**	−0.225	−0.073
Mg^{2+}	**0.928**	−0.060	0.030
Na^{+}	**0.966**	−0.006	0.020
K^{+}	**0.849**	0.042	0.028
Cl^{-}	**0.932**	0.079	−0.001
HCO_3^{-}	0.504	**−0.623**	−0.056
$NO_3^{-}N$	0.145	**0.625**	0.033
SO_4^{2-}	**0.909**	−0.009	0.029
SiO_2	−0.057	**−0.705**	−0.074
Cu	−0.136	0.343	**−0.539**
Mn	0.194	**0.593**	−0.278
Zn	−0.171	0.360	**−0.646**
Cd	−0.120	0.146	−0.213
Pb	−0.138	0.074	**0.604**
Fe	−0.014	−0.002	**0.625**
Al	−0.124	−0.036	0.061
As	−0.051	−0.069	−0.388
Hg	−0.032	−0.101	**0.476**
Se	−0.058	0.123	**0.463**

Extraction method: principal component analysis using Varimax with Kaiser normalization

Values in bold represent 'strongly loaded' (>0.75) or 'moderately loaded' (0.5–0.75) or 'weakly loaded' (<0.5)

Table 8 Rotated component matrix of the main physico-chemical and trace metal parameters

Total variance explained						
Component	Initial eigenvalues			extraction sums of squared loadings		
	Total	% of Variance	Cumulative %	Total	% of Variance	Cumulative %
1	7.213	48.089	48.089	7.213	48.089	48.089
2	2.199	14.660	62.749	2.199	14.660	62.749
3	1.270	8.469	71.218	1.270	8.469	71.218
4	1.054	7.025	78.243	1.054	7.025	78.243
5	1.041	6.939	85.182	1.041	6.939	85.182
6	0.724	4.826	90.008			
7	0.537	3.583	93.591			
8	0.357	2.377	95.968			
9	0.245	1.631	97.599			
10	0.170	1.130	98.729			
11	0.078	0.521	99.250			
12	0.048	0.319	99.569			
13	0.036	0.240	99.809			
14	0.026	0.175	99.984			
15	0.002	0.016	100.000			

Extraction method: principal component analysis

the basin include; silicate $(SiO_4)^{4-}$ dissolutions, ion-exchange reactions, sea aerosol spray and pyrite (FeS) and arsenopyrite (FeAs) oxidations. From Table 3, groundwater within the basin is strongly acidic to neutral, with 81% of boreholes recording pH outside the WHO (2004) Guideline Values for drinking water. The pH levels in groundwater within the basin is due principally to natural biogeochemical processes and the presence of silicates/aluminosilicates found within the basin may probably be responsible for the acid neutralizing potential of groundwater within the basin (Tay et al. 2014). From Fig. 4a, b, the contributions of Na^+, Ca^{2+}, Mg^{2+} and K^+ are 41, 31, 16 and 12%, respectively, while, major anion contribution of HCO_3^-, Cl^- and SO_4^{2-} are 53, 28 and 19%, respectively. The hydrogeochemical transport model Phreeqc for Windows was used to assess the state of saturation of the groundwaters with respect to the major minerals (Table 9). Figure 5, presents the plot of calcite against dolomite saturation indices of groundwater within the Basin. Results show that, groundwaters within the basin are subsaturated with respect to both calcite and dolomite and therefore, represents waters that have come from environments where calcite and dolomite are depleted or where Ca^{2+} and Mg^{2+} exist in other forms. Groundwaters within the basin thus, have not reached equilibrium with the carbonates due to short residence times. Tay et al. (2014), using groundwater geochemistry in determining the origin of major dissolved ions showed that, the chemical composition of groundwater within the basin is the combined chemistry of the composition of water that enters the groundwater reservoir and their reactions with the mineralogy of granitic rocks (biotite, muscovite), schist rocks (biotite, hornblende and actinolite), pyrite and arsenopyrites as the water travels along the mineral surfaces in the pores or fractures of the unsaturated zones and the aquifer. The stability of plagioclase (anorthite) and its secondary weathering products gibbsite, kaolinite and Ca-montmorillonite with respect to groundwater within the Lower Pra Basin showed that, consistent with natural waters with low silica concentrations, most of the groundwaters plot in the kaolinite-stability field, while, the stability of albite and its secondary weathering products gibbsite, kaolinite, and Na-montmorillonite with respect to groundwater within the basin showed that, consistent with natural waters with low silica concentrations most of the groundwaters plot in the kaolinite-stability field indicating that; kaolinite is the most stable secondary silicate mineral phase for the groundwater system. Thus, silicate/aluminosilicate weathering processes may have contributed significantly to the Ca^{2+}, Mg^{2+} and Na^+ concentrations in groundwater within the basin (Tay et al. 2014). Stable isotopes (^2H and ^{18}O) results showed that, the waters emanated principally from meteoric origin with evaporation playing an insignificant role on the infiltrating water (Tay et al. 2014). Tay et al. (2015) assessed the most relevant controls on groundwater quality within the basin using Q-mode hierarchical cluster analysis (HCA). The Q-mode HCA characterized hydrochemical data into four (4) water groups and five (5) subgroups. The

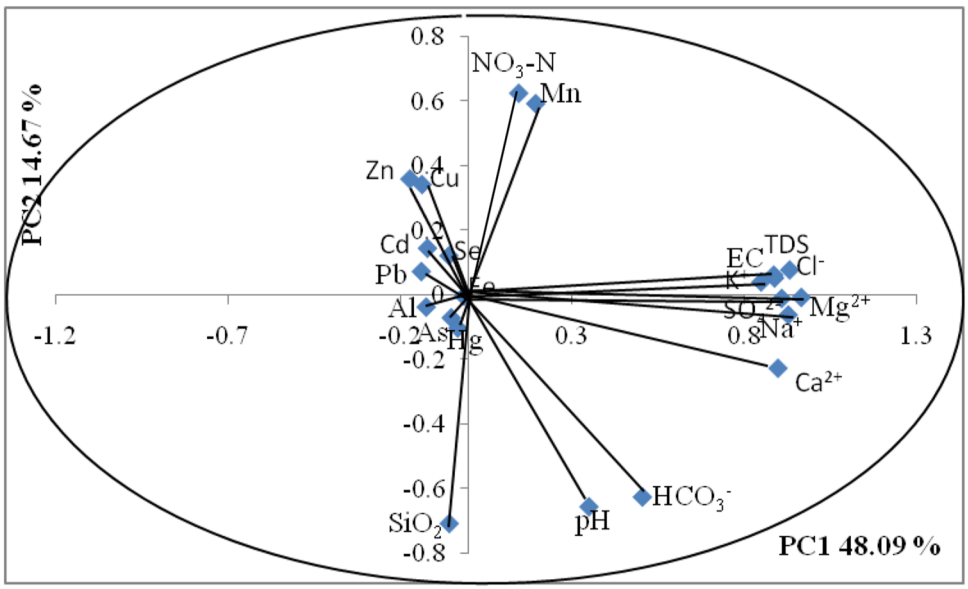

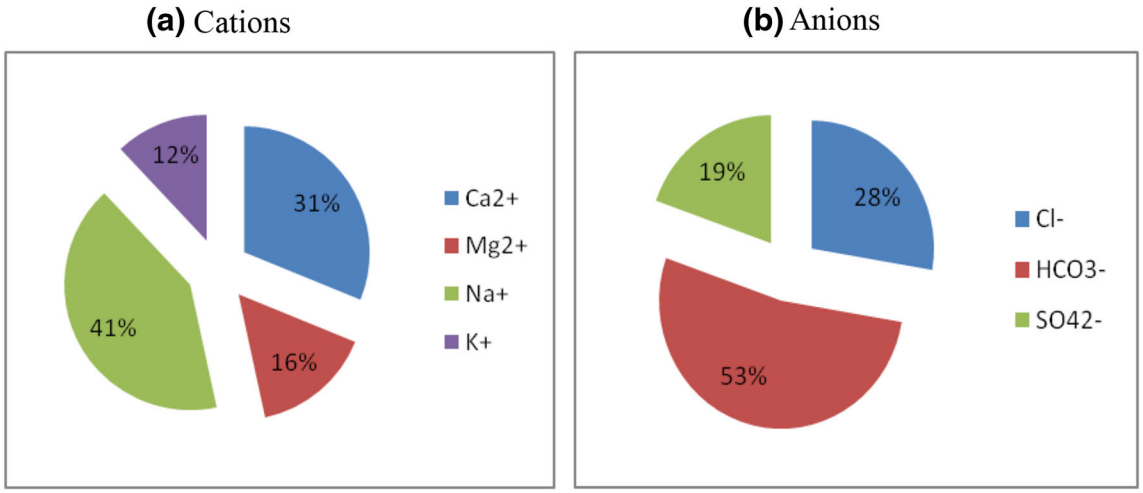

Fig. 3 Loadings and score plot for the first two PCs

Fig. 4 **a**, **b** Relative proportions of the major dissolved constituents in groundwater within the Basin

results from Tay et al. (2015) delineated two main water types- the Na–HCO_3 and Ca–Mg–HCO_3 with Na–Cl and Ca–Mg–Cl as minor water types. The results further showed that, Groups 1 and 2 waters both represents transition zones between Ca–Mg–HCO_3/Na–HCO_3 and Na–Cl/Ca–Mg–Cl type waters and therefore, can be regarded as transition zones between naturally circulating groundwaters which have not undergone pronounced water–rock interaction/aggressive recharging alkali carbonate waters and limited recharging local rain/permanent hard water. Furthermore, Tay et al. (2015) also showed that surface waters within the basin are principally of Na–HCO_3 type waters and therefore are reminiscent of aggressive recharging waters that may potentially be serving as recharge reservoirs to groundwater within the basin. Tay et al. (2015) concluded that, groundwater within the basin perhaps evolves from fresh-Ca–Mg–HCO_3/Na–HCO_3 type waters to permanent hard –Ca–Mg–Cl type waters and limited recharging local rain- Na–Cl type waters along the groundwater flow paths principally due to ion-exchange reactions and that, the surface waters within the basin may potentially be serving as recharge reservoirs to groundwater within the basin. However, Zion Camp area may be serving as discharge areas to groundwater within the basin. PCA using Varimax with Kaiser normalization rotation has resulted in the extraction of three main principal components which identifies the factors influencing each principal components for the main physico-chemical parameters. The three principal components have accounted for approximately 79% of the total variance in the hydrochemical data. Component 1 delineates the main natural processes (water–soil–rock interactions) through which

Table 9 Saturation indices for groundwater calculated using Phreeqc for Windows

Sample source	BHID	*T* (°C)	pH	$Anh_{(SI)}$	$Cal_{(SI)}$	$Dol_{(SI)}$	$Fe(OH)_{3(SI)}$	$Geo_{(SI)}$	$Mel_{(SI)}$	$Gyp_{(SI)}$	$Hem_{(SI)}$	$Sid_{(SI)}$	$SiO_2(a)_{(SI)}$
Assin Nyankomase		28.6	5.1	−0.4	−1.4	−3.4	−3.6	2.3	−5.0	−0.1	6.8	−1.5	−0.8
Assin Nyankomase		27.6	5.6	−0.8	−1.1	−1.9	−1.9	4.0	−4.9	−0.6	10.2	−0.6	−1.1
Assin Nyankomase		29.6	6.1	−1.1	−0.8	−1.0	−0.6	5.3	−5.2	−0.9	12.8	−0.3	−0.5
Sabina	094BU3	28.5	6.1	−0.5	−1.2	−3.0	−3.0	3.0	−5.4	−0.3	7.8	−1.6	−0.7
Ayitey	098BU3	27.6	6.1	−0.3	−0.9	−2.2	−3.4	2.5	−5.4	−0.1	7.2	−1.5	−1.3
Nkrafo	096BU3	27.1	6.1	−0.4	−1.1	−2.1	−3.4	2.5	−5.5	−0.2	7.0	−1.5	−1.1
Nkrafo	099BU3	27.5	7.0	−0.7	−0.2	−0.6	−1.7	4.1	−5.4	−0.5	10.5	−0.3	−1.2
Obirikwaku	405BU2	27.9	6.2	−0.2	−0.6	−1.5	−3.5	2.4	−5.4	−0.1	6.8	−1.4	−1.2
Odumase Camp	407BU2	28.1	6.0	−0.8	−1.5	−3.7	−3.6	2.3	−5.6	−0.6	6.6	−1.7	−0.6
Odumase Camp	246JBU1	27.8	5.9	−0.8	−0.7	−1.4	−0.6	5.3	−5.4	−0.7	12.8	−0.4	−0.4
Obobakokrowa		29.4	5.5	−0.5	−0.4	−1.6	−1.8	4.1	−5.5	−0.3	10.3	−0.8	−1.2
Dwedaama		27.5	6.4	−0.7	−0.9	−1.7	−2.6	3.3	−5.8	−0.5	8.9	−1.4	−1.0
Dwedaama	097BU3	26.5	5.6	−0.2	−0.6	−1.5	−2.6	3.3	−5.2	−0.3	9.0	−0.9	−1.2
Worakese Habitat	101BU3	27.5	5.5	−0.7	−0.1	−0.4	−1.0	4.9	−5.4	−0.5	12.0	−0.1	−0.1
Brofoyedru Habitat		26.4	5.9	−0.6	−0.7	−1.5	−2.9	2.9	−5.3	−0.4	8.2	−0.7	−0.1
Akonfude		26.7	5.8	−0.5	−0.2	−0.8	−0.2	5.7	−4.2	−0.3	13.7	−0.8	−1.2
Akonfude		27.9	5.4	−0.1	−0.4	−1.5	−2.7	3.2	−5.1	−0.1	8.8	−0.8	−1.1
Assin Breku (SDA)	100BU3	27.9	6.1	−0.7	−0.1	−0.1	−0.5	6.4	−4.6	−0.5	15.0	−0.6	−0.4
Assin Breku (Gyidi)	102BU3	26.2	6.9	−0.2	−0.7	−1.4	−0.7	5.2	−0.1	−3.4	12.7	−0.7	−0.9
Assin Breku		27.6	6.2	−0.4	−0.7	−1.9	−3.6	2.3	−0.2	−0.6	6.9	−1.3	−0.3
Techiman No.1	396BU2	26.7	5.5	−0.6	−0.8	−1.8	−3.6	2.3	−0.4	−5.6	6.9	−1.1	−0.7
Kwame Ankra	411BU2	26.5	5.5	−0.3	−0.3	−1.3	0.5	6.3	−0.1	−3.4	15.0	−1.1	−1.0
Ninkyiso		27.6	5.1	−1.1	−0.3	−0.4	0.1	−0.9	−5.4	−0.5	14.1	−0.1	−0.9
Amoakokrom	337BU3	28.4	5.3	−0.4	−0.3	−0.9	−1.7	4.2	−5.7	−0.2	10.6	−1.0	−1.0
Nyamebekyere	339BU3	26.9	5.8	−0.3	−0.2	−0.6	0.1	6.0	−0.1	−4.0	14.3	−0.7	−0.9
Jerusalem	339BU3	26.5	5.4	−0.4	−0.4	−1.2	−2.3	3.6	−0.2	−5.8	9.6	−1.2	−1.0
Antoabasa	0502B1/01/097-01	27.5	5.8	−0.3	−0.4	−1.1	−2.9	−0.1	−5.9	−0.2	8.3	−1.4	−1.1
Antoabasa		27.8	5.6	−0.4	−0.9	−2.0	−1.9	4.0	−0.3	−4.1	10.5	−0.2	−0.9
Bediadua		28.1	6.5	−0.5	−0.6	−1.6	−0.5	5.4	−0.3	−4.0	13.1	−0.6	−1.1
Anum		26.9	5.9	−1.1	−0.3	−0.3	−2.1	3.8	−0.9	−6.5	10.1	−1.0	−0.8
Kyeikurom	086BU3	27.3	5.8	−0.3	−0.3	−0.5	−0.3	5.6	−0.1	−3.9	13.4	−0.7	−0.9
Adukrom	088BU3	26.8	6.4	−0.5	−0.3	−1.1	−2.2	3.7	−0.3	−5.4	9.5	−0.7	−1.0
Subriso		26.8	6.8	−0.2	−0.1	−1.1	−1.5	4.4	−0.2	−4.7	13.0	−0.1	−1.1
Nsuekyir	219BU1	28.0	6.0	−0.5	−0.7	−1.6	−2.2	3.7	−0.3	−4.9	10.9	−0.3	−0.9
Denyease Domeabra	093BU3	27.1	6.7	−0.5	−0.7	−1.6	−2.0	4.0	−0.3	−4.6	9.8	−0.4	−0.9
Twifo Mampong		27.4	6.0	−0.3	−0.4	−0.8	−2.6	3.3	−0.1	−5.3	10.2	−0.1	−1.1
Twifo Mampong		27.9	6.2	−0.3	−0.5	−0.9	−1.4	4.5	−0.1	−4.7	8.7	−0.9	−1.1
Akwa Yaw		26.5	6.2	−0.2	−0.1	−0.1	−0.7	5.2	−0.1	−4.8	11.2	−0.3	−1.0
Breman	260BU2	27.4	6.7	−0.1	−0.7	−1.6	−3.2	2.7	−0.1	−4.7	12.6	−0.1	−1.2
Breman		27.9	6.6	−0.3	−0.5	−0.9	−2.7	3.2	−0.1	−5.1	7.8	−0.7	−1.1
Twifo Agona	236BU2	26.8	5.9	−0.1	−0.5	−1.1	−2.6	3.3	−0.1	−4.9	8.6	−0.6	−1.1
Zion Camp	014BU3	26.4	6.8	−1.0	−0.1	−0.1	−3.2	2.7	−1.2	−4.5	7.6	−0.9	−1.2

Table 9 continued

Sample source	BHID	*T* (°C)	pH	$Anh_{(SI)}$	$Cal_{(SI)}$	$Dol_{(SI)}$	$Fe(OH)_{3(SI)}$	$Geo_{(SI)}$	$Mel_{(SI)}$	$Gyp_{(SI)}$	$Hem_{(SI)}$	$Sid_{(SI)}$	$SiO_2(a)_{(SI)}$
Somnyamekordur	138BU1	27.7	6.7	−0.2	−0.3	−0.6	−0.1	5.9	−0.1	−3.4	8.8	−0.7	−1.1
Somnyamekordur	033BU3	27.3	5.8	−0.2	−0.3	−0.7	−1.4	4.5	−0.1	−4.6	14.0	−1.2	−1.0
Atu Kurom		28.3	5.6	−1.1	−0.3	−0.7	−0.2	5.7	−0.9	−4.7	11.3	−0.1	−0.9
Subreso		26.4	6.5	−1.2	−0.1	−0.1	1.6	7.5	−1.0	−4.7	13.6	−0.7	−0.8
Gromsa	032BU3	27.5	6.4	−0.3	−0.1	−0.1	−1.7	4.2	−0.1	−5.3	17.2	−1.1	−0.8
Anyinase Ankase	030BU3	27.3	5.9	−1.4	−0.1	−0.4	0.4	6.3	−1.2	−5.8	10.6	−0.4	−1.0
Sienkyem	24/B/32/1	26.6	5.4	−0.3	−0.4	−0.3	−0.4	4.2	−1.3	−5.0	14.6	−0.3	−0.7
Sienkyem	24/B/32/1	26.4	5.5	−0.1	−0.2	−0.6	−1.9	4.0	−0.1	−4.9	14.6	−0.7	−1.1
Mamponso	24-B-85-1	27.2	5.8	−0.3	−0.1	−0.7	−0.3	5.6	−0.1	−4.7	10.1	−0.4	−0.8
Essamang		26.8	5.3	−1.4	−0.8	−0.1	−1.8	4.0	−0.3	−1.1	13.4	−0.1	−1.0
Mampong	22/D/73-1	27.8	5.5	−0.3	−0.1	−0.3	−1.4	4.5	−0.7	−4.5	8.8	−0.4	−0.7

SI saturation index, *Anh* anhydrite, *Cal* calcite, *Dol* dolomite, *Hem* Hematite, *Sid* Siderite, *Geo* goethite, *Gym* gypsum, *Mel* Melantherite, $SiO_{2(a)}$ amorphous silica

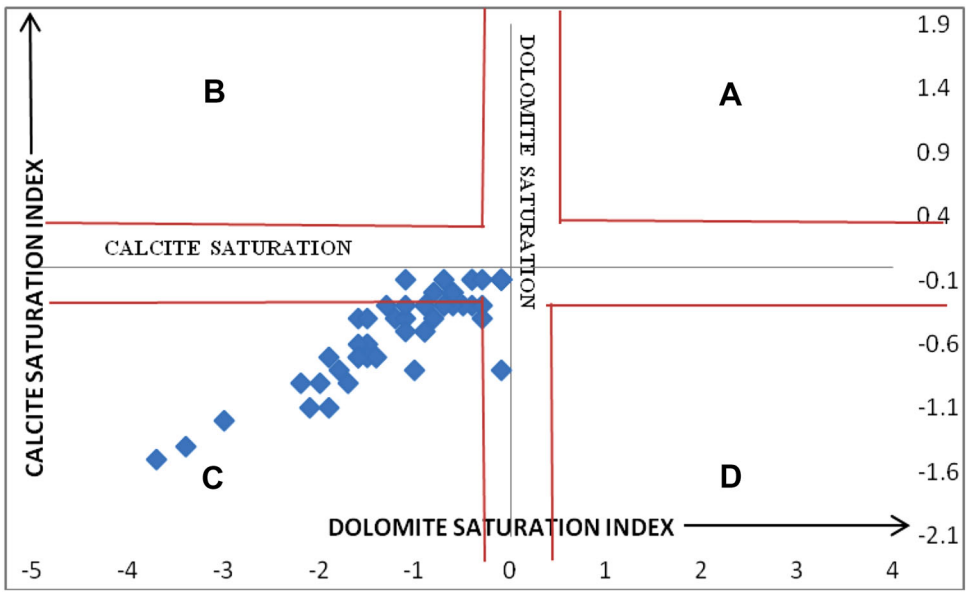

Fig. 5 A plot of calcite against dolomite saturation indices of groundwater within the Basin

groundwater within the basin acquires its chemical characteristics, Component 2 delineates the incongruent dissolution of silicate/aluminosilicates, while Component 3 delineates the prevalence of pollution principally from agricultural input as well as trace metal mobilization in groundwater within the basin.

Conclusion and recommendations

The application of multivariate statistical technique for groundwater assessment within the Lower Pra Basin have shown that, correlation matrix of major ions revealed expected process-based relationships derived mainly from the geochemical processes, such as ion exchange and silicate/aluminosilicate weathering within the aquifer. Spearman's Correlation matrix and PCA results show the possible existence of a process-based relationship between Cu^{2+} and Zn^{2+} ($r = 0.92$; $p < 0.05$). Three main principal components influence the water chemistry and pollution of groundwater within the basin. The three principal components have accounted for approximately 79% of the total variance in the hydrochemical data. Component 1 delineates the main natural processes (water–soil–rock interactions) through which groundwater within the basin acquires its chemical characteristics, Component 2 delineates the incongruent dissolution of silicate/aluminosilicates, while, Component 3 delineates the prevalence of pollution principally from agricultural input as well as trace metal mobilization in groundwater within the basin. In terms of

trace metal mobilization, the study show that though, the trace metals reflects a common source of mobilization, where Pb, Fe, Hg and Se concentrations are high, Cu and Zn concentrations are low. The loadings and score plots of the first two PCs show grouping pattern which indicates the strength of the mutual relation among the hydrochemical variables. In terms of proper management and development of groundwater within the basin, communities where intense agriculture is taking place should be monitored and protected from agricultural activities especially, where inorganic fertilizers are used by creating buffer zones. Monitoring of the water quality especially the water pH is recommended to ensure continuous acid neutralizing potential of groundwater within the basin thereby, curtailing further trace metal mobilization processes in groundwater within the basin.

Acknowledgements The authors are grateful to the Government of Ghana through the Council for Scientific and Industrial Research-Water Research Institute (CSIR-WRI) for providing financial assistance and analytical facilities for this PhD study. We are also grateful to Mr. Harrison Komladjei a Principal Draughtsman of the CSIR-WRI, for the maps of the study area.

References

Ahialey EK, Serfoh-Armah Y, Kortatsi BK (2010) Hydrochemical analysis of groundwater in the Lower Pra Basin. J Water Resour Prot 2:864–871

Ahmed SM, Blay PK, Casto SB, Coakley GJ (1977) Geology of (¼)° field sheets Nos. 33 Winneba NE 59, 61 and 62 Accra SW, NW and NE. Ghana Geological Survey Bulletin No. 32

Alberto WD, Del Pilar DM, Valeria AM, Fabiana PS, Cecilia HA, De Los Angeles BM (2001) Pattern recognition techniques for the evaluation of spatial and temporal variations in water quality. A case study: Suquia River basin (Cordoba-Argentina). Water Res 35:2881–2894

American Public Health Association (APHA) (1998) Standard methods for the examination of water and wastewater, 20th edn. American Public Health Association, Washington, DC

Appelo, Postma (1999) Geochemistry, groundwater and pollution. AA Balkema/Brookfield, Rotterdam

Barcelona M, Gibb J P, Helfrich JA, Garske EE (1985) Practical guide for groundwater sampling. Ilinois State Water Survey ISWS Contract Report 37

Bayitse R (2011) Pattern of pollution at the Lower Basin of River Pra, Unpublished MPhil Thesis. Environmental Science Programme, University of Ghana

Briz-Kishore BH, Murali G (1992) Factor analysis for revealing hydrochemical characteristics of a watershed. Environ Geol Water Sci 19(1):3–9

Catchment-Based Monitoring Project in Ghana-National IWRM Plan (2010) EU-Funded monitoring groundwater resource occurrence and their quality in the Tano and Pra River Basins with surface water quality monitoring in the South-western, Coastal and Volta River Basins. CSIR-WRI Quarterly Consultancy Report Covering 01/04/2010 to 30/06/2010. Water Resources Commission

Claasen HC (1982) Guidelines and techniques for obtaining water samples that accurately represent the quality of an aquifer. US Geological Survey Open File Report 82-1024, 49 pp

Clark ID, Fritz P (1997) Environmental isotopes in hydrology. Lewis, Boca Raton

Cloutier V, Lefebvre R, Therrien R, Savard MM (2008) Multivariate statistical analysis of geochemical data as indicative of the hydrogeochemical evolution of groundwater in a sedimentary rock aquifer system. J Hydrol 353:294–313

Dalton MG, Upchurch SB (1978) Interpretation of hydrochemical facies by factor analysis. Groundwater 16:228–233

Dappah S, Gyau-Boakye P (2000) Hydrologic framework and borehole yields in Ghana. Hydrogeol J 8:405–416

Das JD, Nolting RF (1993) Distribution of trace metals from soils and sewage sludge's Abay refluxing with aqua regia. Analyst 108:277–285

Dickson KB, Benneh GA (1980) New geography of Ghana. Longman, London

Duah AA (2007) Groundwater contamination in Ghana. In: Xu Y, Usher B (eds) Groundwater pollution in Africa. Taylor and Francis Group, London, pp 57–64

Farnham IM, Johannesson KH, Singh AK, Hodge VF, Stetzenbach KJ (2003) Factor analytical approaches for evaluating groundwater trace element chemistry data. Anal Chim Acta 490(1):123–138

Fetter CW (1994) Applied hydrology, 3rd edn. Prentice-Hall, New York

Freeze RA, Cherry JA (1979) Groundwater. Prentice-Hall Inc, New Jersey

Gűler C, Thyne GD, McCray JE, Turner AK (2002) Evaluation of graphical and multivariate statistical methods for classification of water chemistry data. Hydrogeol J 10:455–474

Hem JD (1989) Study and interpretation of the chemical characteristics of natural water, 3rd edn. US Geological Survey Water Supply Paper 2254

Hounslow AW (1995) Water quality data analysis and interpretation. Lewis Publishers, Boca Raton

Jiang Y, Wu Y, Groves C, Yuan D, Kambesis P (2009) Natural and anthropogenic factors affecting the groundwater quality in the Nandong karst underground river system in Yunan, China. J Contam Hydrol 109:49–61

Junner NR, Hirst T, Service H (1942) Tarkwa Goldfield. Memoir No. 6. Gold Coast Geological Survey

Kesse GO (1985) The mineral and rock resources of Ghana. A.A. Balkema, Rotterdam

Kim JO, Mueller CW (1978) Introduction to factor analysis: what is and how to do it. Quantitative applications in the social sciences series. Sage, Newbury Park

Kim JM, Kim RH, Lee JH, Cheong TJ, Yum BW, Chang HW (2009) Multivariate statistical analysis to identify the major factors governing groundwater quality in the coastal area of Kimje, South Korea. Hydrol Process 19(6):1261–1276

Kortatsi BK (2007) Hydrochemical framework of groundwater in the Ankobra Basin, Ghana. Aquat Geochem 13:41–74. doi:10.1007/s10498-006-9005-4

Lawrence FW, Upchurch SB (1982) Identification of recharge areas using geochemical factor analysis. Groundwater 20:680–687

Liu CW, Lin KH, Kuo YM (2003) Application of factor analysis in the assessment of groundwater quality in a Blackfoot disease area in Taiwan. Sci Total Environ 313:77–89

Morris BL, Lawrence ARL, Chilton PJC, Adams B, Calow RC, Klinck BA (2003) Groundwater and its susceptibility to degradation. A global assessment of the problem and options for management. Early Warning and Assessment Report Series, R S 03-3. United Nations Environmental Programme, Nairobi, Kenya

Piper AM (1944) A graphic procedure in the geochemical interpretation of water analyses. Am Geophys Union Trans 25:914–923

Sandaw MY, Duke O, Banoeng-Yakubu B, Abdul AS (2012) A factor model to explain the hydrochemistry and causes of fluoride enrichment in groundwater from the Middle Voltaian Sedimentary Aquifers in the Northern Region, Ghana. ARPN J Eng Appl Sci 7(1). ISSN 1819-6608

Satheeshkumar P, Anisa Khan B (2011) Identification of mangrove water quality by multivariate statistical analysis methods in Pondicherry coast, India. Environ Monit Assess. doi:10.1007/s10661-011-2222-4

Schoeller H (1965) Qualitative evaluation of groundwater resource. In: Methods and techniques of groundwater investigation and development. UNESCO, pp 54–83

Shrestha S, Kazama F (2007) Assessment of surface water quality using multivariate statistical techniques: a case study of the Fuji river basin, Japan. Environ Model Softw 22(4):464–475

Siever R, Woodward N (1973) Sorption of silica by clay minerals. Geochim Cosmochim Acta 37:1851–1880

Stiff HA Jr (1951) The interpretation of chemical water analysis by means of patterns. J Petrol Technol 3:15–17

Subba Rao N (2002) Geochemistry of groundwater in parts of Guntur district, Andhra Pradesh, India. Environ Geol 41:552–562

Subbarao C, Subbarao NV, Chandu SN (1995) Characterization of groundwater contamination using factor analysis. Environ Geol 28(4):175–179

Suk H, Lee KK (1999) Characterization of a groundwater hydrochemical system through multivariate analysis: clustering into groundwater zones. Groundwater 37(3):358–366

Tay CK, Kortatsi BK, Hayford E, Hodgson IO (2014) Origin of major dissolved ions in groundwater within the Lower Pra Basin using groundwater geochemistry, source-rock deduction and stable isotopes of ^{2}H and ^{18}O. Environ Earth Sci 71:5079–5097. doi:10.1007/s12665-013-2912-z **ISSN: 1866-6280**

Tay CK, Kortatsi B, Hayford E, Hodgson I (2015) Hydrochemical appraisal of groundwater evolution within the Lower Pra Basin, Ghana: a hierarchical cluster analysis (HCA) approach. Environ Earth Sci 73:3579–3591. doi:10.1007/s12665-014-3644-4 **ISSN 1866-6280**

Vega M, Pardo R, Barrato E, Deban L (1998) Assessment of seasonal and pollution effects on the quality of river water by exploratory data analysis. Water Res 32:3581–3592

Woocay A, Walton J (2008) Multivariate analyses of water chemistry: surface and groundwater interactions. Groundwater 46(3):437–449

Zhang Q, Li Z, Zeng G, Li J, Fang Y, Yuan Q, Wang Y, Ye F (2009) Assessment of surface water quality using multivariate statistical techniques in red soil hilly region: a case study of Xiangjiang watershed, China. Environ Monit Assess 152:123–131. doi:10.1007/s10661-008-0301-y

Zhou F, Guo HC, Liu Y, Jiang YM (2007) Chemometrics data analysis of marine water quality and source identification in Southern Hong Kong. Mar Pollut Bull 54(6):745–756